

50-MeV BEAM MONITORING AT THE ZERO GRADIENT SYNCHROTRON (ZGS)\*

R. L. Martin and R. C. Trendler  
Argonne National Laboratory  
Argonne, Illinois 60439

ABSTRACT

The 50-MeV beam monitoring system at the ZGS has been made operational. It consists of vertical and horizontal nondestructive beam distribution measurements at four points along the beam transport line between the linac and the ZGS, and a horizontal position measurement in the middle of the achromatic injection system. The results are displayed on the computer display scope. The beam distribution measurements allow calculation of the beam emittance and can be displayed on a pulse-to-pulse basis to indicate changes in the emittance or beam steering. The position measurement in the achromatic system is an indication of the average energy of the beam. Initial operating results with this system are discussed.

Description of the System

The locations of the elements of the system, with respect to the quadrupoles and achromatic bending magnets of the 50-MeV beam line, are shown in Fig. 1. The nondestructive Profile and Position System (PAPS) detectors each consist of 10 elements horizontally and 10 elements vertically for ion collection from ionization of the residual gas. The elements are arranged on 0.2" centers to give a 2" span to the measurement. Switching elements activate either the horizontal or vertical set and the same amplifiers are used for both. Details of the PAPS detectors and investigations of their properties have been published.<sup>1-4</sup> The  $\pi$  electrode at the center of the achromatic bending magnet system is a simple two-triangular element electrode from which horizontal position information is obtained by sum and difference ratios. It also operates by ion collection and is nondestructive. A beam toroid measures the beam intensity after the last achromat.

Position measurements from the first pair of PAPS detectors indicate beam alignment directly from the linac since the steering magnets (not shown in Fig. 1) are placed between the second detector and the first quadrupole magnet. In principle,

---

\*Work performed under the auspices of the U.S. Atomic Energy Commission.

emittance can be determined from beam distribution measurements at three locations if they are properly placed with respect to the waists of the beam envelope. In practice, however, use of a fourth distribution to obtain a least squares fit gives a more reproducible result. The position measurement at the center of the achromatic bending magnet system provides a measurement of the average energy of the beam. This is true only if the first two magnets are at their design currents and the beam is centered in horizontal position and angle at the entrance to the first magnet. These conditions are not a serious drawback, however, because the interest in this monitoring system is not to determine absolute values but to observe deviations from good operating conditions.

### Displays

One computer program collects the information from all of the PAPS detectors on two successive pulses (one for horizontal distributions, the second for vertical distributions), and presents the results for any selected detector on the display scope. Figure 2 shows such a display in which the top curve is the horizontal distribution and the lower curve is the vertical distribution. The points are present data and can be automatically updated every second pulse or held to allow the operator to examine the distributions from all four detectors on the same pulse. The curves drawn by the computer come from stored data obtained from the PAPS system during operation of another program. They assist the operator in visually observing whether conditions (beam center or width) have changed. This program averages the readings of the elements of each PAPS detector for 15 successive pulses in each plane and computes a least squares fit to a five-parameter curve of the form  $y = A e^{-B(x-C)^D} + E$ . The parameters for each curve are stored and recalled to draw the curves displayed in Fig. 2.

Figure 3 shows the display obtained from the third computer program. The bottom curve is the integrated beam toroid current and the top five curves are the beam position obtained from the  $\pi$  electrode. Each curve represents a different 20  $\mu$ sec interval during the pulse. All curves represent the last 100 pulses of the linac whether or not this display is being used. The decrease of injected beam current observed on the lower trace was caused by adjustment of the linac rf gradient reference voltage, and one observes no change of the position of the beam through the achromats by this adjustment.

The program which computes the distribution curve parameters also produces two other useful displays. After receiving input of the currents in the steering magnets and quadrupoles, the emittance and orientation of the ellipse in phase space in

both planes is computed. Using this information, the calculated beam envelopes along the 50-MeV transport line (Fig. 4), and central ray steering, including steering effects by the quadrupoles (Fig. 5), are presented. The four data points on each of these computed curves are the measured data from the PAPS detectors. At this point the operator can insert new currents for any of the elements into the computer and observe the resulting changes without actually affecting the 50-MeV beam operation. Similar flexibility on matching problems with the 12-BeV external proton lines has proven most useful once the operator has gained sufficient experience to guess at simultaneous changes of several magnet currents to produce a desired effect.

One further display available to the operators (though not a part of this monitoring system) is the histogram of accelerated intensity of the ZGS (Fig. 6). Each point represents one pulse of the ZGS and the histogram can contain  $\sim 1700$  points. Therefore, depending on the ZGS repetition rate, the operator can observe the ZGS intensity history for a period of about 1-1/2 h. Changes in average intensity and in stability are easily recognizable. It was this consideration which mainly stimulated the development of the present nondestructive 50-MeV monitoring system; namely, when changes in accelerated intensity or stability occur, can the operator determine whether such changes are due to the injector system or to effects in the main ring? At the present time calling up any other display destroys this intensity record. Programming is nearly complete, however, to store updated intensity information on disc so that one will be able to recall the complete histogram at will.

### Results

The system described, complete with computer displays, was made operational in April shortly before the coil failure of the ZGS. During the shutdown for replacement of the coil, a high gradient column was installed on the preaccelerator. Stable operation of the injector and the ZGS with accelerated beam currents in excess of  $2 \times 10^{12}$  protons/pulse was achieved near the end of August. Investigation of the utility of the 50-MeV monitoring system has, therefore, been rather limited and the results quite incomplete. Some comments can be made at this time however.

From the computer displays one can easily observe shifts of beam centers of less than 100 mils when steering magnets are adjusted. Adjustment of one of the quadrupole currents by 5% produces easily visible and expected changes of beam distributions, both horizontal and vertical, at a downstream PAPS detector. These visual observations by the operator are greatly aided by using the curves shown on the displays for reference. The detector output amplitudes are directly proportional to the

pressure in the beam line. In order to preserve the visual monitoring sensitivity of the operator it is necessary to recompute the curves when pressure changes occur.

Steering changes of the beam are also observed by the adjustment of quadrupole currents, indicating that the beam center does not pass through the magnetic center of the quadrupoles. This result is not necessarily surprising in view of the overall uncertainty in beam alignment shown in the ray plot of Fig. 5. In particular, the calculated vertical steering of the beam, which does not fit the measurements of the last two PAPS detectors, leads to a predicted vertical injection angle into the ZGS of 2.4 mrad. This injection angle is outside of the acceptance of the ZGS. More detailed measurements, and perhaps realignment of the quadrupole magnets, will be required to resolve these questions. Another result, very likely related to the above, is that the beam is off center at the  $\pi$  detector by  $0.4''$ . While the beam can be brought to the proper location at this point by adjustment of the currents in all of the achromatic magnets, the captured and accelerated beam of the ZGS are reduced.

During the investigations of this system the ZGS operators have continued to adjust all parameters to keep the ZGS operating stably with good accelerated intensity. Over a two-week span little change was noticed in the beam distributions or steering in the 50-MeV beam line. On one occasion, however, when the ZGS was retuned after a shutdown and operating well, the beam angle from the exit of the linac was decidedly different and compensated further downstream by different values of the 50-MeV steering magnets. In an effort to locate the cause, all parameters of the source, preaccelerator, and 750-keV transport line were investigated. Only the 750-keV steering magnets produced a steering effect at 50 MeV. By adjustment of these magnets we were able to return the 50-MeV beam line to its previous steering conditions as seen on the PAPS detectors. Continued adjustment in the same direction produced no continuation in the direction of the change, but a reversal! When all parameters, including the 50-MeV steering magnets, were returned to values existing before the shutdown the ZGS intensity was back to normal, a condition that the ZGS operator states was not true at turnon. Resolution of questions such as these may help stabilize the operation of the ZGS.

The computed envelope curve of Fig. 4 fits the widths determined from all of the PAPS detectors reasonably well and gives some confidence in the reliability of the "emittance" measurement. The actual value of the emittance is subject to some interpretation and is a strong function of the percentage of beam included. We define our emittance measurement as that containing 99% of the beam represented by the fitted curve. The value obtained  $\sim 4 \pi$  cm-mrad in both planes, is not inconsistent with more

detailed measurements made previously with slits. At this point the actual value is of secondary importance. The real importance lies with the reproducibility of the measurement and the meaning of any change. A series of five emittance measurements made over a two-week operating period gave good reproducibility of the vertical emittance ( $< 5\%$  variation). The variation of the horizontal emittance, however, varied somewhat more ( $\sim 20\%$ ). We have not yet been able to determine whether these variations are real or merely represent the stability and resolution of the monitoring system.

### Conclusions

The 50-MeV monitoring system of the ZGS seems to hold a great deal of promise for improving ZGS operations. For example, a serious malfunction or wrong connection of any component in the injector line could be quickly spotted by the monitoring system. It is clear, however, that considerably more experimentation is needed to determine the capabilities of the system for pinpointing variations of the injector system to which the ZGS is sensitive.

In its short life the monitoring system has already raised a number of questions that must be resolved, some of which have been discussed above. In addition, it could prove more useful for beam diagnostics of steering and matching than for the troubleshooting function for which it was designed. The hope remains, however, that by use of this system we will learn how to reproduce "good" injector beam conditions which lead to high stable intensity in the ZGS, and thereby attain an average accelerated intensity closer to the peak achieved as well as shorten the turnon time after an extended shutdown.

### Acknowledgements

The authors have carried out this investigation for the purpose of making this monitoring system a useful tool for operation of the ZGS. Development of the detectors and the electronics was initiated by W. DeLuca and M. Shea and completed by R. Sanders. Software development and data presentation were carried out by G. Concaildi and R. George. Special credit belongs to S. Marcowitz who was project leader and contributed many of the concepts employed in this system.

### References

- <sup>1</sup>W. DeLuca and M. Shea, Argonne National Laboratory, A Nondestructive Linac Beam Density Profile Monitor, 1968 Proton Linear Accelerator Conference, Upton, New York, May 20-24, 1968, Published as BNL 50120 (C-54), part 1, pp. 190-197.

- <sup>2</sup>W. DeLuca, Argonne National Laboratory, Beam Detection Using Residual Gas Ionization, 1969 Particle Accelerator Conference, Washington, D.C., March 5-7, 1969, Published in IEEE Transactions on Nuclear Science, (June, 1969), vol. NS-16, no. 3, part I, pp. 813-822.
- <sup>3</sup>R. A. Sanders, "50-MeV Beam Profile and Position System (PAPS)," Report No. RAS-6, August 1, 1969, Argonne National Laboratory, Accelerator Division, Argonne, Illinois.
- <sup>4</sup>G. Concaildi, R. George, S. Marcowitz, R. Sanders, "A Nondestructive Measurement of Phase-Space Properties of the 50-MeV Proton Beam Between the Linac and the ZGS," Report No. GC/RG/SM/RS-1, December 3, 1969, Argonne National Laboratory, Accelerator Division, Argonne, Illinois.

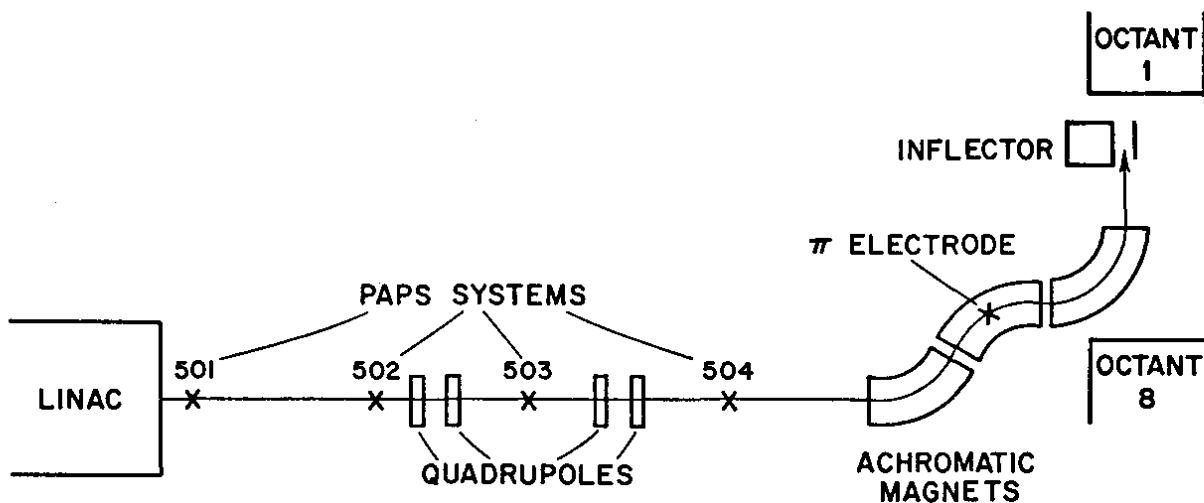


Fig. 1. 50-MeV transport line of the ZGS (not to scale).

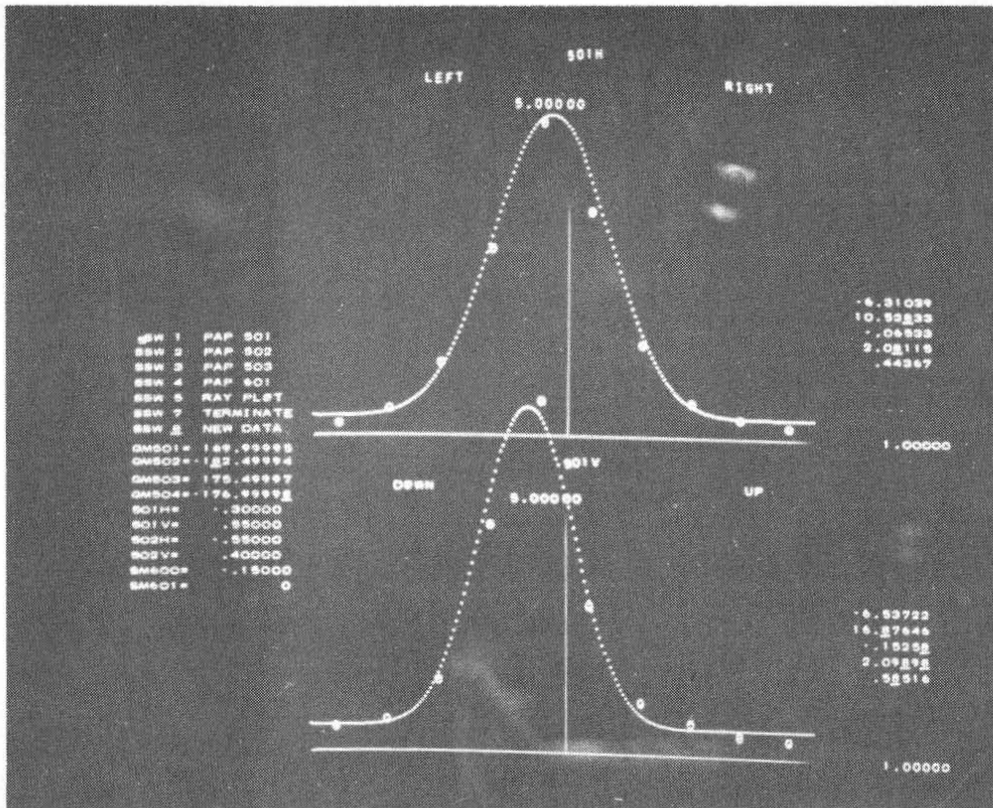


Fig. 2. PAPS 501 horizontal and vertical beam profiles.

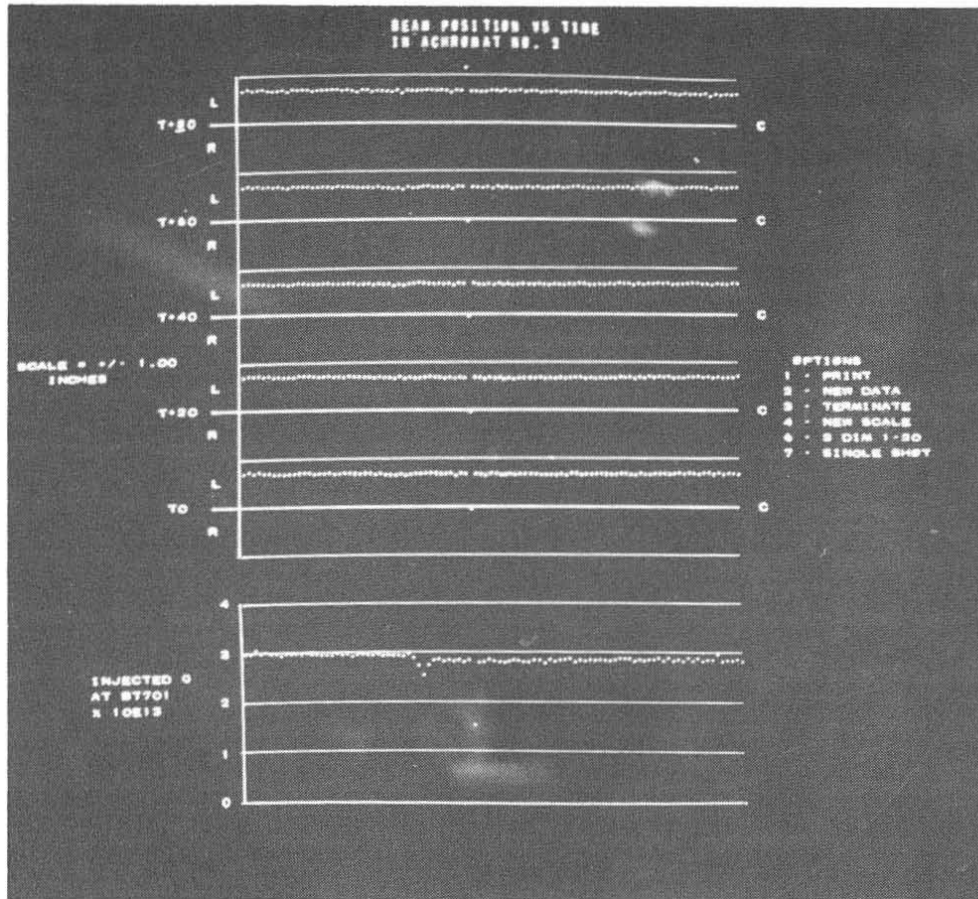


Fig. 3. 100-pulse histogram.  
 a. (Lower curve) Integrated injected intensity after achromate.  
 b. (Upper five curves) Beam position at  $\pi$  electrode each 20  $\mu$ sec of beam pulse.



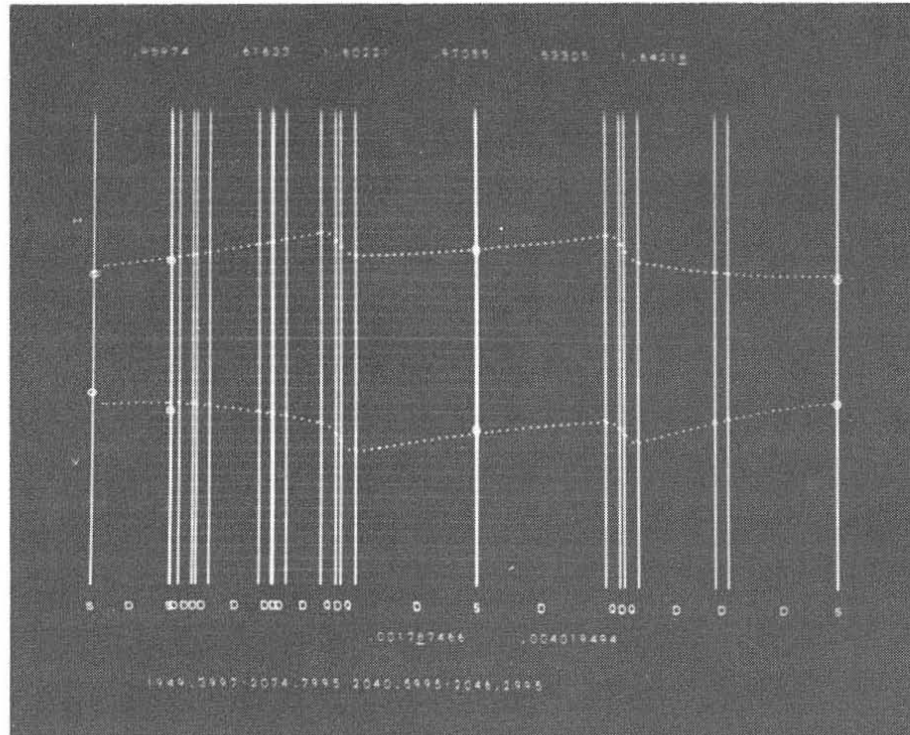


Fig. 4. Computed horizontal and vertical beam envelopes of 50-MeV transport line.

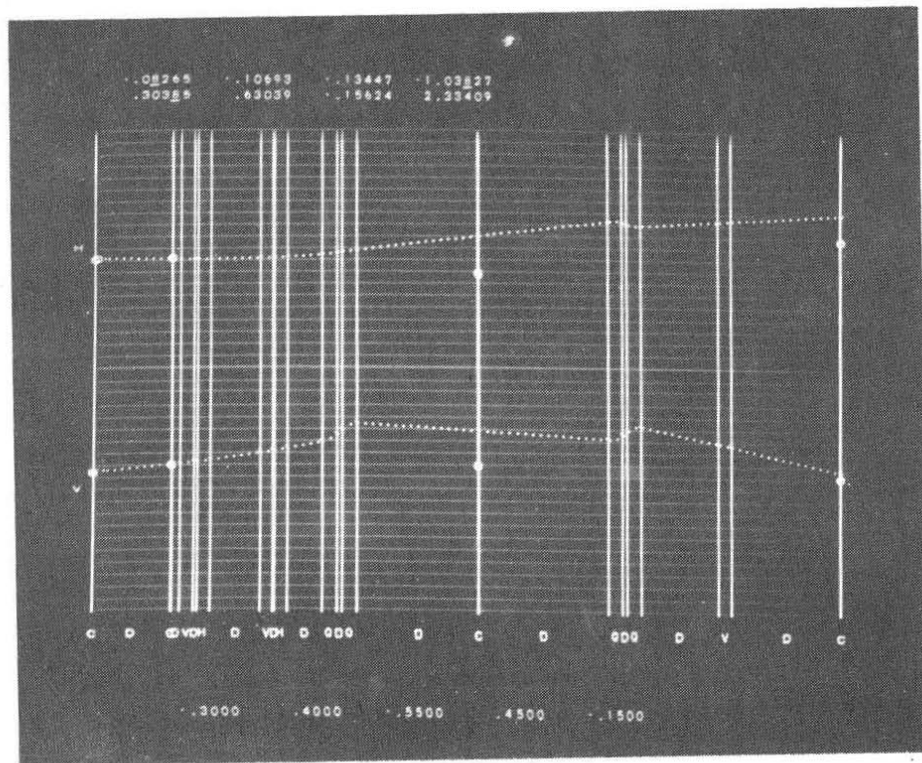


Fig. 5. Computed central-ray steering profiles in horizontal and vertical planes.

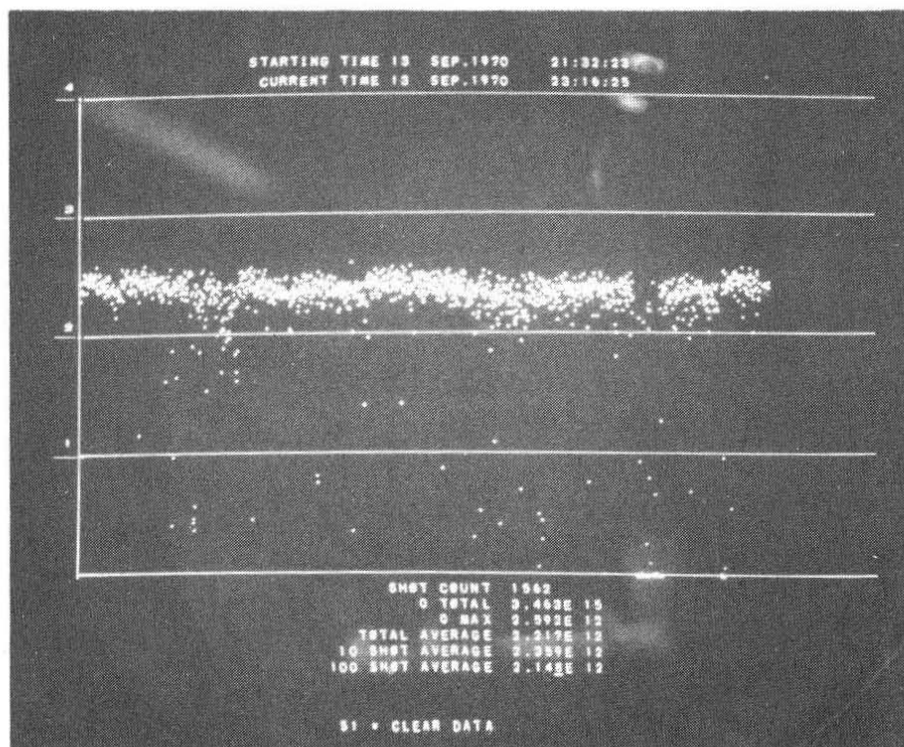


Fig. 6. Histogram of ZGS accelerated intensity in units of  $10^{12}$  protons/pulse.